platelets

http://www.tandfonline.com/iplt
ISSN: 0953-7104 (print), 1369-1635 (electronic)

Platelets, 2018; 29(5): 476–485
DOI: https://doi.org/10.1080/09537104.2017.1332365

Taylor & Francis
Taylor & Francis Group

ORIGINAL ARTICLE

Enhanced adhesion of blood platelets to intact endothelium of mesenteric vascular bed in mice with streptozotocin-induced diabetes is mediated by an up-regulated endothelial surface deposition of VWF – *In vivo* study

Tomasz Przygodzki[1], Marcin Talar[1], Hassan Kassassir[1], Lukasz Mateuszuk[2], Jacek Musial[3], & Cezary Watala[1]

[1]*Department of Haemostasis and Haemostatic Disorders, Medical University of Lodz, Lodz, Poland,* [2]*Jagiellonian Centre for Experimental Therapeutics (JCET), Jagiellonian University, Krakow, Poland, and* [3]*Synevo Central Laboratory, Department of Pathology, Lodz, Poland*

Abstract

Numerous *in vitro* experiments have confirmed that a dysfunctional endothelium is characterized by, *inter alia*, a higher affinity for binding of platelets and leukocytes. However, there is still no direct evidence for greater interaction between platelets and intact endothelium in *in vivo* animal models of diabetes. Therefore, the present study examines the pro-adhesive properties of endothelium change *in vivo* as an effect of streptozotocin (STZ)-induced diabetes and the role of two key platelet receptors: GPIb-IX-V and GPIIb/IIIa.

Mice of C57BL strain with streptozotocin-induced diabetes were used in the study. Flow cytometry was used to assess basal activation and reactivity of platelets. Adhesion of platelets to the vascular wall was visualized with the use of intravital microscopy in mesentery. The contribution of GPIIb/IIIa and GPIb-IX-V was evaluated by the injection of Fab fragments of respective antibodies. The integrity of the endothelium and vWf expression were evaluated histochemically. Basal activation and reactivity of platelets in streptozotocin-diabetic mice were elevated. Blood platelets adhered more often to the vascular wall of diabetic mice than nondiabetic animals: 11.9 (6.4; 32.8) plt/min/mm^2 (median [IQR]) vs 2.7 (1.3; 6.4) plt/min/mm^2. The injection of anti-GPIbα antibodies decreased the number of adhering platelets from 89.5 (34.0; 113.1) plt/min/mm^2 (median [IQR]) in mice treated with isotype antibodies to 3.1 (1.7; 5.6) plt/min/mm^2 in mice treated with blocking antibodies. The effect of GPIIb/IIIa blockage was not significant. Immunohistochemistry revealed a higher expression of vWF in the endothelium of STZ mice, but no substantial changes in endothelial morphology were detected.

To conclude, the study shows that the platelets interact more frequently with the mesenteric vascular bed in mice with 1-month STZ-induced diabetes than in healthy mice. These interactions are mediated via platelet GPIb-IX-V and are driven by increased expression of vWF in endothelial cells.

Keywords

Endothelial dysfunction, diabetes, intravital microscopy, platelet adhesion

History

Received 23 August 2016
Revised 24 April 2017
Accepted 10 May 2017
Published online 25 July 2017

Introduction

Besides other abnormalities, a dysfunctional endothelium is characterized by a higher affinity for binding of platelets and leukocytes, and this has been proven in numerous *in vitro* studies, as well as in the *in vivo* studies based on various animal models of endothelial dysfunction [1–5]. This pro-inflammatory state of a dysfunctional endothelium is considered to be a primary cause for the development of atherosclerosis [6]. It is suggested that the interaction between platelets and the inflamed endothelium facilitates the adhesion of monocytes to the vascular wall, which is recognized as a first step in the development of atherosclerotic lesions.

Diabetes mellitus (DM) is a metabolic condition associated with the dysregulation of the cardiovascular system. The inflammation of the endothelium and increased activation of blood platelets are strongly associated with this disease in humans [7]. Both of these abnormalities are also reproduced in animal models of diabetes. Increased basal activation and reactivity of platelets [8–12] and endothelial dysfunction [13–16] have been shown in animal models representing human models of type I and type II diabetes. However, no direct evidence exists which suggests that the interactions between platelets and the intact endothelium *in vivo* are enhanced in an animal model of diabetes. Therefore, the aim of the present study is to examine how the pro-adhesive properties of the endothelium change in streptozotocin-induced diabetes in an *in vivo* model, one of the most often used rodent models of DM corresponding to

Correspondence: Tomasz Przygodzki, Department of Haemostasis and Haemostatic Disorders, Medical University of Lodz, Mazowiecka 6/8, Lodz 92-215, Poland. E-mail: tomasz.przygodzki@umed.lodz.pl

Color versions of one or more of the figures in the article can be found online at www.tandfonline.com/iplt

human type 1 diabetes. The study also determines the role of two platelet receptors, which are recognized as being chiefly involved in this process, namely GPIb-IX-V and GPIIb/IIIa.

Materials and methods

Materials

Male C57BL mice aged 8–12 weeks were obtained from the Center of Experimental Medicine, Medical University of Bialystok (Bialystok, Poland).

Blood platelet-specific DyLight488-labeled anti-GPIbβ antibodies for *in vivo* labeling, isotype antibodies for blocking experiments (non-immune rat IgG), FITC- and PE-conjugated rat anti-CD41/61, PE-conjugated rat anti-CD62P, PE-conjugated JON/A antibodies (rat anti-active complex GPIIb/IIIa), FITC-conjugated rat anti-von Willebrand factor antibodies were purchased from Emfret Analytics (Eibelstadt, Germany). Fab fragments of the monoclonal anti-GPIbα antibodies Xia.B2 clone and anti GPIIb/IIIa Leo.H4 clone were a kind gift from Emfret. Streptozotocin (STZ) and protease-activated receptor-4 (PAR-4) activating peptide (AYPGKF) were purchased from Sigma (St. Louis, MO, USA). Mouse von Willebrand factor A2 Elisa Kit was obtained from Abcam (Cambridge, UK). Materials for histochemistry were purchased from Sigma, Menzel Gläser (Braunschweig, Germany). Normal goat serum and Cy3-conjugated secondary goat-anti-rabbit antibody for immunohistochemistry were purchased from Jackson Immuno (West Grove, PA, USA) and primary rabbit-anti-mouse von Willebrand factor antibody was from Abcam (Cambridge, UK).

Methods

Induction of diabetes

The studies were approved by the Local Ethical Committee on Animal Experiments, Medical University of Lodz (approval number 65/LB572/2011). Experimental diabetes was induced in C57BL 8-week-old mice by intraperitoneal injection of 200 mg/kg b.w STZ in 0.1 mol/l citrate buffer (pH 4.5). Control mice were injected with a vehicle. STZ-diabetic animals, in which blood glucose values exceeded 16.6 mmol/l 7 days after STZ injection, were recruited to the study. Measurements of glucose levels were conducted daily.

Analysis of platelet count and size

Blood was collected on K_2EDTA pH 7.3, from the inferior vena cava. Platelet count and size were then analyzed with a sciI Vet abc Plus + veterinary hematological analyzer (Horiba, Kyoto, Japan).

Assessment of platelet adhesion to vascular wall with the use of *in vivo* microscopy

Thirty days after injection, the mice were anesthetized, injected with platelet-specific fluorescent anti-GPIbβ antibodies at a dose of 0.1 μg/g b.w. and placed on the stage of an upright microscope equipped with saline immersion objectives. The antibodies do not interfere with the interaction between GPIbα and vWF. The mesentery was exteriorized and fixed in a chamber allowing constant superfusion with saline. Imaging was carried out for 40 seconds with an exposure time of 200 ms in at least three sites of the mesenteric vascular bed in each mouse. In the experiment testing the effect of blocking antibodies, the anti-GPIα Fab fragments, anti-GPIIb/IIIa Fab fragments, or nonimmune rat IgG antibodies (control), were injected into the tail vein at a dose of 60 μg per mouse.

The analysis of platelet adhesion was performed with the use of ImageJ software supported with the MTrackJ plugin [17].

Measurements of blood platelet adhesion to von Willebrand factor *in vitro*

Blood platelet adhesion was assessed with the use of the VenaFlux platform (Cellix, Dublin, Ireland). The channels of a Vena8 Fluo + biochip were coated with von Willebrand factor (20 μg/ml) overnight at 4°C and blocked with BSA (1 mg/ml) for 1 hour at 4°C. The biochip was mounted on a thermically controlled stage of an inverted AxioVert microscope (Carl Zeiss, Oberkochen, Germany) assuring a constant temperature of 37°C throughout the experiment. Prior to measurements the channels were washed with PBS. The blood was collected on heparin from the inferior vena cava and fluorescent anti-GPIbβ antibodies were added: the same as those used for intravital microscopy. After a 5-minute incubation, the blood was perfused through the channel at 20 dynes/cm^2 for 5 minutes. Images were taken using a 40x objective at an exposure time of 2 seconds at five different sites along the channel using a filter set dedicated for FITC. Platelets, which did not change their position during exposure (2 seconds), were imaged as discoid objects, while those displaced in this timeframe were imaged as smears. The results of the experiment were quantified by counting only the discoid objects in five defined areas in each of the images.

Flow cytometry analysis

The blood was centrifuged and cellular blood components were suspended in Tyrode's buffer as described previously [10]. The activation of circulating platelets, and the platelet reactivity in response to PAR-4 activating peptide (AYPGKF), at final concentrations of 20 or 100 μM, were evaluated by measuring the expression of the specific surface membrane antigens CD62P (P-selectin) and activated GPIIb/IIIa complex, as well as the binding of endogenous von Willebrand factor to the platelet surface.

Platelets were gated on the basis of the binding of anti-GPIIb/IIIa antibodies. Flow cytometric measurements of platelet surface membrane antigens were performed with the use of light scatter (threshold 200) and fluorescence gates set on the platelet fraction. The green or orange fluorescence of the stained platelets was recorded for FITC (filter transmitting at 530 nm, with a bandwidth of 30 nm) and PE (filter transmitting at 585 nm, with a bandwidth of 42 nm), respectively, using the FACS Canto II instrument (BD Biosciences, San Jose, CA) with the excitation set at 488 nm. At least 10 000 cells were analyzed per sample. All data were processed using FACS/Diva ver. 6.0 software (BD Biosciences, San Jose, CA).

The percent fractions of specific fluorescence-positive platelets were evaluated after subtracting the binding of nonspecific isotype mouse IgG_1. The gate for isotype control was set to 2%. Results were presented as the percent fractions and MFI values for CD62P-, activated $\alpha_{IIb}\beta_3$- and vWf-positive platelets. Additionally, platelet size measurement was used to distinguish between cohorts of newly produced (larger, referred to as "fresh") or exhausted (smaller, referred to as "old") platelets in the population of single platelets, as well as between single and "clumped" platelets (CD41/61-positive cells) in resting, non-stimulated blood.

The diameter of the platelets in blood samples was determined using a standard curve prepared with FSC calibration beads covering the following size ranges: 0.5, 1, 2–2.4, 3–3.4, 5–5.9, 7–7.9, 8–12.9, 13–17.9 μm.

It should be borne in mind that the use of artificial beads for any size-related calibrations is imprecise, as the beads and platelets display different refractive indices. Therefore, our intention was not to determine the exact size of platelets in blood samples, but rather to reveal the differences in the cohorts of newly produced and exhausted platelets and in the forming of "larger"

platelet aggregates/clumps, between diabetic and healthy mice, that would reflect the activation state of circulating platelets in tested groups of animals.

Concentration and functionality of vWF in plasma

Whole blood, collected as described above, was centrifuged at 800 × g for 15 minutes at 4°C. Von Willebrand factor was assayed in plasma with the use of enzyme-linked immunosorbent assay according to manufacturer's instructions.

Twenty-five microliters of blood collected from a healthy mouse was diluted 25-fold with Tyrode's buffer, spun down (900 × g, 5 minutes), the supernatant was discarded and the cellular blood components were reconstituted in 25-fold times diluted plasma from either STZ-diabetic or nondiabetic mouse. Flow cytometry analysis of vWF binding to platelets in response to ristocetin (at a final concentration of 12.5 mg/ml) was conducted as described above.

Histochemistry and immunohistochemistry

To create histochemical images, formaldehyde-fixed (4% in PBS) and paraffin-embedded mesenteries were cut to small sections (4 μm). The sections were mounted on superfrost slides, then dewaxed with xylene, hydrated, and boiled in the antigen retrieval solution buffer for 10 minutes. All sections were counterstained with Meyer's hematoxylin. Imaging was performed with the use of the AxioVert inverted microscope (Carl Zeiss, Oberkochen, Germany) with a standard color CCD camera (magnitude 400x).

To perform vWF staining, the mesenteries were cut into 5 μm-thick cross-sections using Accu-Cut SMR 200 rotary microtome (Sakura Finetek, Tokyo, Japan) and collected on polylysine-covered microscopic slides. The cross-sections were de-paraffinized, using a Leica ST5020 multistaining station (Leica, Wetzlar, Germany), and incubated in a citrate buffer (95°C/30 minutes.) according to the standardized heat-induced epitope retrieval (HIER) protocol. To minimize nonspecific antibody binding, slides were pre-incubated in blocking solution containing 5% normal goat serum, 2% dry milk, and 0.1% Triton X-100 for 45 minutes. Primary rabbit-anti-mouse von Willebrand factor antibody was applied for a 1-hour incubation period, followed by a 30-minute incubation with Cy3-conjugated secondary goat-anti-rabbit antibody. Finally, the nuclei were counterstained with Hoechst 33258 fluorescent dye. The images of mesenteric vessels were taken using an AxioObserver D1 inverted fluorescent microscope and AxioCam HRm monochromatic digital camera (Carl Zeiss, Oberkochen, Germany). Image analysis was performed semi-automatically using Axio Vision 4.8 software (Carl Zeiss, Oberkochen, Germany).

Statistics

Data are expressed as mean ± SD for normally distributed variables, or as median and interquartile range (IQR: lower [25%] to upper [75%] quartile) otherwise. The normal distributions of data were verified with Shapiro–Wilk's test and variance homogeneity tested with Levene's test. Unpaired Student's *t*-test was employed to reason on the significance of differences when comparing two independent groups with distributions not departing from normality. In some cases, for normally distributed data when the assumption of homoscedasticity was violated, we used the planned comparisons with the Welch's test. When normality assumption was violated, we made an attempt to transform the raw data using the Box-Cox transformation. If the assumptions were still not met, the significance of differences was tested with Mann–Whitney's *U* test. When comparing multiple data sets we used one-way or two-way block ANOVA (with relevant *post-hoc* multiple comparisons tests), and in the case when our data were not satisfying the criterion of normality and/or variance homogeneity, the Kruskal–Wallis' test followed by post-hoc Dunn's test for multiple comparisons was used. In addition, due to relatively small sample sizes and the low statistical power of the estimated inferences in some calculations, we employed the resampling bootstrap technique (1000–10 000 iterations) to determine how likely it would be to obtain the revealed differences due to a pure chance. In such circumstances we refer to the bootstrap-boosted test statistics (1000 iterations) instead of the classical approach. For some variables, the overall population of data was decomposed into two exponentially modified Gaussian partial distributions (subpopulations) with the use of the Data Mining-assisted generalized cluster analysis by EM (expectation–maximization) algorithm.

Statistical analysis was performed using Statistica v. 12.5 and Resampling Stats Add-in for Excel v.4.

Results

Streptozotocin-induced diabetes

Postprandial glucose levels on the day of the experiment were significantly higher in mice treated with STZ than those treated with citrate: 30.6 ± 1.3 mmol/l vs 8.0 ± 4.6 mmol/l (mean ± SD), respectively; $p < 0.001$ (unpaired, one-sided, Student's *t*-test), $n = 11$.

The numbers and sizes of platelets in control and diabetic mice subjected to hematological analysis

The numbers of platelets were 948 ± 63 x 10^3 plt/μl in control mice and 883 ± 131 x 10^3 plt/μl (mean ± SD) in STZ mice. The difference was not statistically significant (Student's *t*-test). However, the mean platelet volume was significantly lower in control mice, 4.9 (4.8; 4.9) fL, than in STZ diabetic mice, 5.1 (4.9; 5.2) fL (median [IQR]), ($P_{bootstrap} < 0.03$), as indicated by the bootstrap-boosted Mann–Whitney's *U* test ($n = 9$).

Interaction of blood platelets with vascular wall

Analyses of the video sequences revealed two modes of interaction between the platelets and the vessel wall: some of the objects attached to vascular wall and remained at the same place for a period of time while others did not remain at one site for subsequent frames of the video sequence. The latter group possibly included platelets rolling or sliding on the surface of vascular wall (Figure 1). To quantify the results, the video sequences were analyzed frame by frame. Each fluorescent object which could be distinguished from the background was traced with the aid of the software. The distance covered by each object and the linear velocity of the objects displaced in the movie sequence were calculated. The number of platelets interacting with the vessel wall was normalized for a duration of a movie sequence and for an area of the vessel. Mean values for particular mouse were calculated based on the data obtained for the video sequences recorded in this mouse. A total number of platelets interacting with the vessel wall were significantly higher in the STZ than in the control mice: 20.9 (12.5; 65.4) plt/mm^2/min in non-STZ-diabetic mice *vs.* 59.9 (30.9; 127.1) plt/mm^2/min (median [IQR]) in the STZ-diabetic mice (one-tailed $p < 0.05$ as revealed by Mann–Whitney *U* test; $n = 11$ for control and $n = 12$ for STZ-diabetic mice). To honestly evaluate these outcomes, we have to be aware however, that there is a source of inaccuracy in counting of all of the interacting objects. The faster an object moves, the more difficult is to identify it. The accuracy of counting of fast moving objects is definitely a source of error, as it strongly

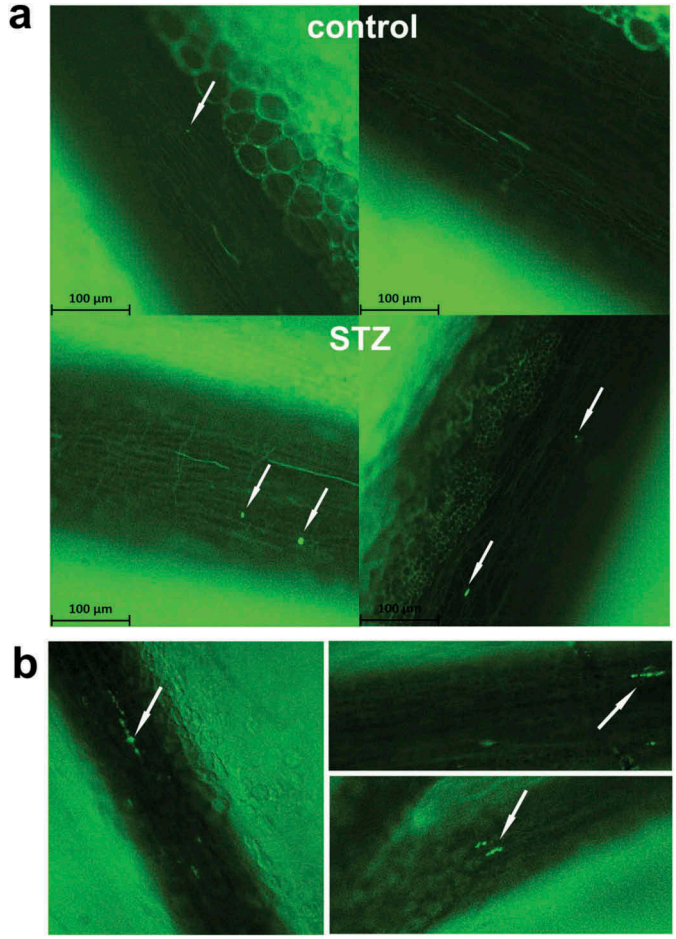

Figure 1. *In vivo* imaging of blood platelet adhesion to the vascular wall in control and STZ-diabetic mice. Mice were injected with anti-GPIbβ antibodies conjugated with DyLight488. Observations were carried out in the mesentery vascular bed under an upright fluorescence microscope equipped with a water immersion objective. (a) Two representative frames are shown for control and STZ group. Adherent platelets are seen as dots, while streaks represent those platelets, which displaced during the exposure period. (b) Objects observed occasionally in STZ mice which appearance was similar to the "strings" of vWF decorated with blood platelets.

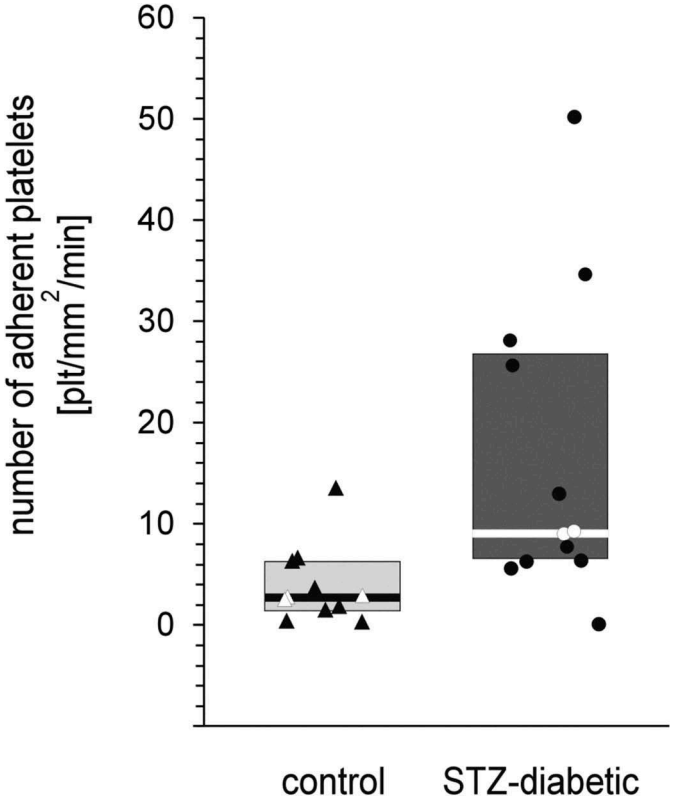

Figure 2. The number of platelets immobilized for at least 400 ms on mesenteric vascular wall in control and STZ-diabetic mice. Results shown as median (horizontal line) with interquartile range (box) and raw data. Significance of differences tested with Mann–Whitney *U* test. ** $p < 0.01$; $n = 11$ for control and $n = 12$ for STZ-diabetic mice.

depends on (*i*) the quality of movie sequence, which can differ between the fields, and on (*ii*) the level of efficacy of platelet staining, which can vary between mice. Thus, in our opinion a more accurate solution is to define a clear criterion that defines which objects are counted. Thus, to do so, we have arbitrarily categorized of all the observed events into two groups: (a) adhering platelets, which attached and did not displace for at least two frames (400 ms) and (b) sliding platelets. In the case of the platelets that were not immobilized for longer than 400 ms, we decided to compare the distributions of their velocities keeping in mind the limitations described above (Figure 3).

The number of platelets, which at least transiently adhered to the vessel wall, was significantly higher in mice with streptozotocin-induced diabetes (Figure 2). The duration of a single event of adhesion was not significantly different between the two groups: 14.0 (0.7; 21.7) s (median [IQR]) in non-STZ-diabetic animals *vs*. 20.7 (16.0; 29.9) s in STZ-diabetic animals ($n = 11$ for control and $n = 12$ for STZ-diabetic mice). As shown on a histogram of velocity distribution (Figure 3a), the velocities of platelets were lower in STZ-diabetic than in nondiabetic mice, indicating that the platelets in these animals were more likely to interact with vascular wall.

Since the distribution of velocities in control group appeared bimodal, we employed the Data Mining-assisted cluster analysis to decompose the overall population of data into two exponentially modified Gaussian partial distributions (Figure 3b). The median value of the second cluster appeared to be shifted more toward lower velocities in STZ-diabetic mice than in nondiabetic animals, which further confirms that platelets in STZ animals are more prone to interact with the vascular wall.

Microscopic observations also revealed in STZ mice the occasional appearance of objects that could be identified as blood platelets forming strings on vWF released by the activated endothelium (Figure 1) as described in the literature [18, 19].

In the experiment testing the effect of blocking antibodies on the platelet adhesion, platelets which were adherent at the beginning of recording were excluded from the calculation. The rationale for this decision was that these platelets could have adhered prior to injection of blocking antibodies, and so could have been potential false negative observations regarding the effectiveness of the blocking antibodies. As shown in Figure 4, the number of platelets transiently adhering to the vascular wall was significantly lower in mice injected with anti-GPIbα blocking antibodies. In mice treated with anti-GPIIb/IIIa blocking antibodies the number of adhering platelets was lower but did not reach statistical significance. The use of blocking antibodies was found to have no effect on the velocities of the sliding platelets.

Flow cytometry analysis of platelet activation, reactivity, and size

Flow cytometry analysis revealed that the circulating platelets demonstrated higher activation in STZ-diabetic mice than control

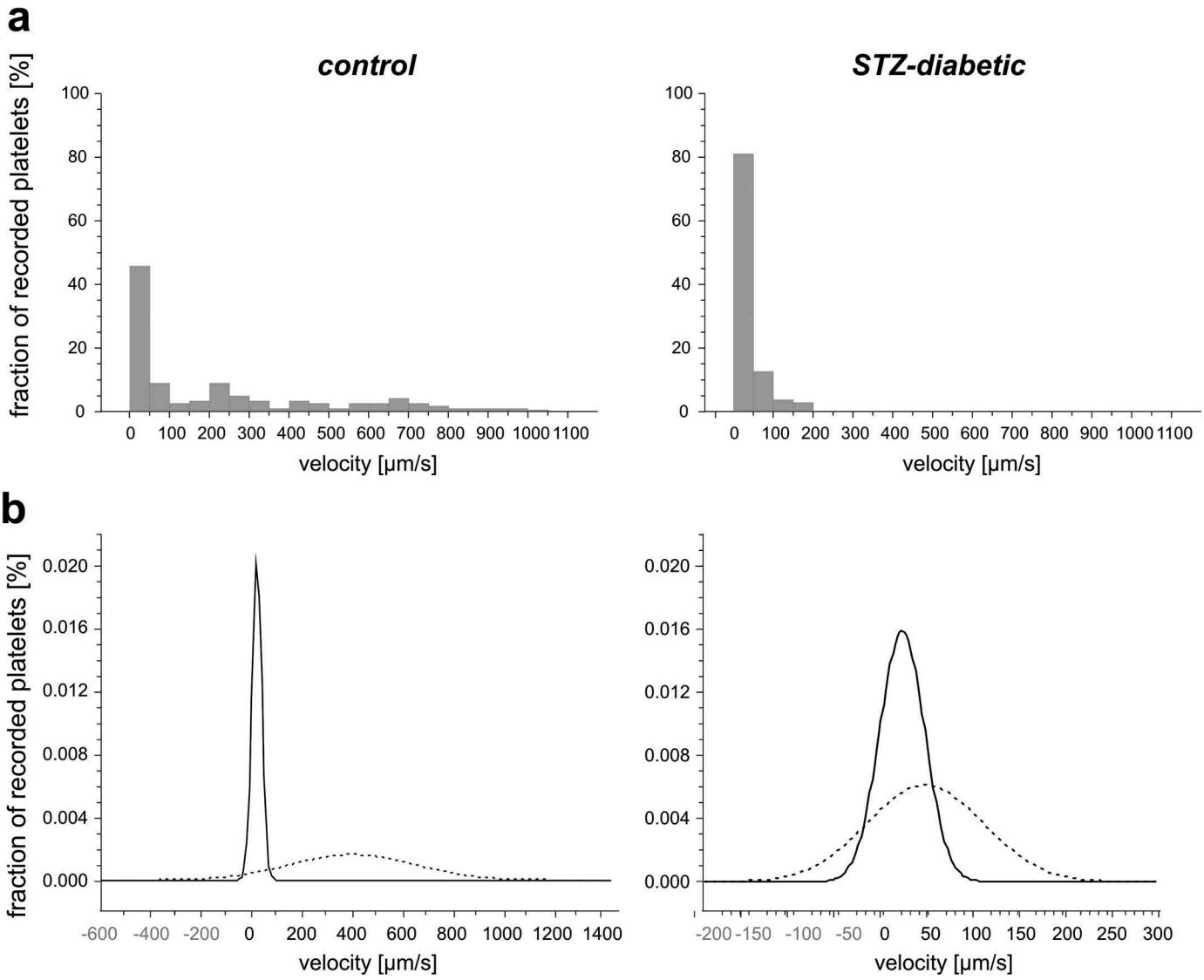

Figure 3. Quantification of platelet velocities. (a) Histogram showing distribution of platelet velocities in control and STZ-diabetic mice; blood platelets, which were immobilized on mesenteric vascular wall for a period shorter than 400 ms, were considered as sliding on a vessel wall; the median of velocities with interquartile range was equal to 62.5 (18.9; 306.1) μm/s in control group and to 11.8 (0.4; 36.3) μm/s in STZ-diabetic mice; the analysis of differences between groups was conducted for mean velocities calculated for each mouse with a blocked ANOVA, $p < 0.0001$; $n = 11$ for control and $n = 12$ for STZ mice. (b) The decomposition of the exponentially modified Gaussian curves circumventing the histograms reveals two populations of platelets in terms of their adhesive properties. Probability density function of the timespan of adhesion for both groups is given by Poisson distribution: $\frac{\mu^x e^{-\mu}}{x!}$, where μ is respective median velocity and x is a velocity for which the probability is calculated.

mice (Figure 5), as evidenced by increased expression of CD62P, active GPIIb/IIIa, and bound vWF. Upon the stimulation of platelets with AYPGKF (PAR-4 agonist), we obtained significantly higher platelet response in STZ-diabetic as compared to vehicle-injected mice, for all the tested markers of platelet activation (Figure 5). This discrimination between diabetic and nondiabetic mice was apparent regardless of the concentration of PAR-4 activating peptide.

As described above, our microscopic observations revealed occasional events which could be interpreted as the formation of platelet aggregates on vWF released by activated endothelium. Therefore, the next part of the study examined the distribution of smaller objects (referred to as normal (single) blood platelets or normoplatelets) and larger objects (referred to as platelet clumps or platelet aggregates) in blood from control and STZ animals. It was found that the proportion of the fraction of "platelet aggregates" to the fraction of "normoplatelets" was significantly higher in STZ mice, clearly indicating that "platelet aggregates" were much more abundant in diabetic animals (Figure 5). With regard to the difference between the fraction of vWF-positive platelets, the binding of vWF to platelets was approximately equally distributed between "normoplatelets" and "aggregates" in control animals, but was significantly higher in the subpopulation of platelet "aggregates" in STZ animals (Figure 5).

Adhesion of blood platelets to vWF in flow conditions

To evaluate whether the enhanced propensity of platelets to interact with vWF in STZ mice was an intrinsic feature of these platelets the next part of the study measured their ability to interact with immobilized vWF under flow conditions. The number of blood platelets which remained adhered to a surface coated with von Willebrand factor for at least 2 seconds did not differ significantly between control and STZ diabetic mice (Figure 6).

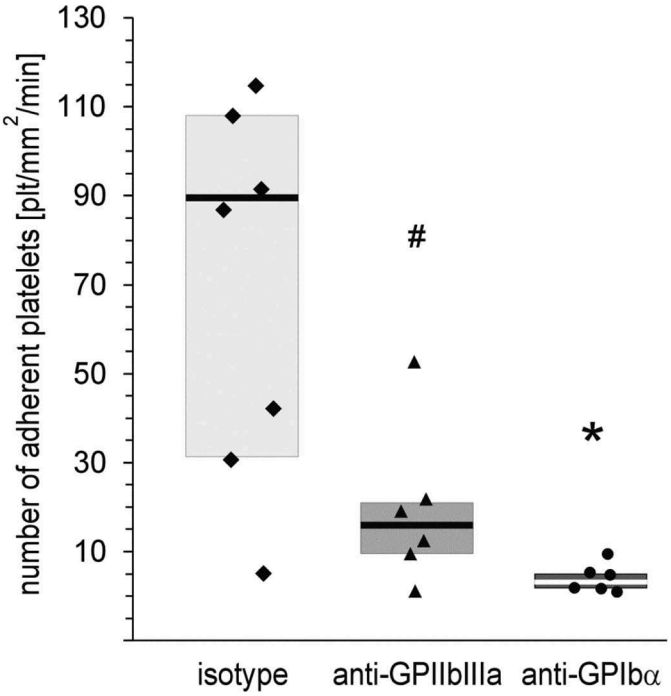

Figure 4. The effect of blocking antibodies on the number of platelets immobilized for at least 400 ms on the mesenteric vascular wall in streptozotocin-injected (STZ) mice. Results shown as median (horizontal line) with interquartile range (box) and raw data; $n = 7$ for isotype antibodies injected mice, $n = 6$ for anti-GPIIb/IIIa and $n = 6$ for anti-GPIbα. Significance of differences tested as planned comparisons with one-tailed Welch's test, followed by the bootstrap-boosted one-tailed Student's *t*-test with the Bonferroni's correction for multiple comparisons (in parentheses); $^{*}p_{\text{Welch}} < 0.02$ ($p_{\text{bootstrap}} = 0.0086$), $^{\#}p_{\text{Welch}} = 0.0614$ ($p_{\text{bootstrap}} = 0.0718$).

Von Willebrand factor concentration and functionality assay in plasma

The concentration of soluble vWF in plasma was 88.7 ± 28.7 ng/ml (mean ± SD) in control mice and 106.6 ± 38.2 ng/ml (mean ± SD) in STZ mice. The difference was not statistically significant ($p = 0.079$; one-tailed Student's *t*-test; $n = 17$ for control and $n = 14$ for STZ mice).

Ristocetin caused a significant increase in the binding of vWF to platelets from plasma: 75.8 ± 9.5 % after ristocetin *vs*. 13.0 ± 0.9 % (mean ± SD) in the non-treated plasma. However, the binding in the STZ and the control plasma was not significantly different: 78.2 ± 8.1 % in the control and 72.7 ± 5.0% (mean ± SD) in plasma of STZ diabetic mice.

Histochemistry

Fluorescent immunohistochemical staining of vWF in mesenteric vessels demonstrated significantly higher expression of the protein in the endothelium of STZ-diabetic mice (Figure 7).

The histochemical staining of mesenteric blood vessels did not reveal any substantial changes in endothelial morphology, such as loss of integrity and detachment of endothelial cells from basement membrane, in STZ-diabetic mice compared to other animal models of dysfunctional endothelium [20, 21] (Figure 8). A subtle edema of some of the endothelial cells was observed in selected specimens of STZ-diabetic mice; this was not observed in the control mice and could be possibly interpreted as a sign of dysfunction (see Additional file 1).

Discussion

The paper is the first to show that blood platelets in a mouse model of diabetes are more likely to interact with an intact vascular wall than those in nondiabetic animals. The interaction of platelets with the endothelium *in vivo* in diabetic animals has not been previously examined but it has been shown that chronic hyperglycemia leads to endothelial activation and renders it more adhesive for leukocytes. Increased rolling of leukocytes was observed *in vivo* in the mesentery in rats with 2-week STZ diabetes [22].

Our recorded interactions were generally short-lasting, the platelets were transiently adhering or sliding on the vessel wall. Although a higher frequency of platelet interactions with the endothelium was observed in diabetic than nondiabetic mice, the difference between the median durations of a single interaction in these two groups was of marginal significance. These findings show that 1-month STZ-induced diabetes results in moderate alteration of adhesive properties of the vascular wall in the mesentery. When compared to another mouse model of metabolic disorder associated with endothelium dysfunction, the effects observed in our experiment were relatively mild. In ApoE–/– mice, which spontaneously develop atherosclerosis, Massberg et al. report much more numerous events of firmly adhering platelets [6] in sites which are more susceptible to the development of atherosclerotic lesions, i.e., the bifurcation of the common carotid artery. The increased binding of platelets in this model was observed before any histological evidence of atherosclerotic lesions could be found. Similarly, in our model, histological examination of the mesenteric vascular bed did not reveal any apparent deterioration of the endothelial layer or any formation of atherosclerotic plaque.

The increased frequency of interactions assessed in our studies could be explained by enhanced basal activation and reactivity of blood platelets, as revealed by flow cytometry. It is accepted that one of the main proteins involved in the interaction of a platelet with the activated endothelium is fibrinogen, which is bound to VCAM and ICAM on endothelial cells [23]. The platelets of the STZ-diabetic mice in the present study demonstrated increased expression of the active form of GPIIb/IIIa which binds fibrinogen. This is in agreement with studies published previously [11, 24]. Another pair of proteins thought to contribute to the interaction between platelets and the inflamed endothelium is the binding of GPIb to vWF or P-selectin present on the endothelium.

To verify which of the two platelet receptors contributed to the greatest extent in our model, the effect of respective blocking antibodies on platelet adhesion was examined. To avoid thrombocytopenia, known to be caused by the injection of entire IgG [25], Fab fragments were used. While the enhanced propensity of interactions was decreased by GPIb receptor blocking, GPIIb/IIIa blocking effect was not significant. The lack of significance might be an effect of a low sample size, thus we do not exclude the contribution of GPIIb/IIIa in these enhanced interactions. In a study of ApoE–/– mice, Massberg et al. noted that inhibition of GPIIb/IIIa reduced the firm adhesion of platelets, defined as lasting more than 20 seconds, but had no effect on transient interactions. In turn, GPIb inhibition significantly decreased both firm and transient interactions [6]. Hence, the contribution of GPIIb/IIIa to the interactions seems to be more prominent in the carotid artery of ApoE–/– mice than these observed in our model. It could be suggested that in our model of endothelial dysfunction is not severe enough to

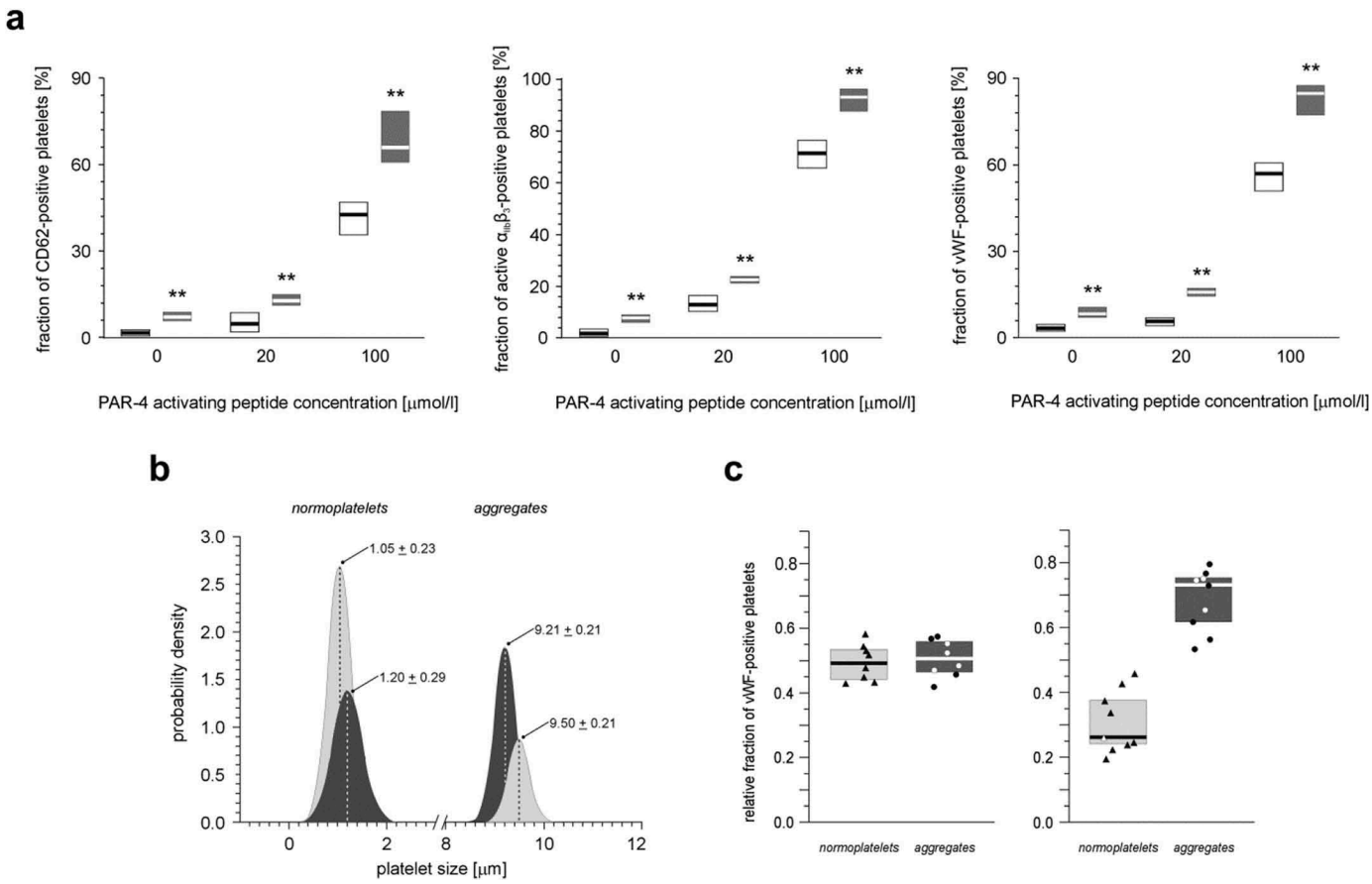

Figure 5. Flow cytometry analysis of changes of selected markers of platelet activation in response to protease-activated receptor-4 (PAR-4) activating peptide (AYPGKF). (a) Concentration "0" represents the basal activation of platelets. Results are shown as median (horizontal line) with interquartile range (box). The significance of differences between the control (light grey) and STZ-diabetic (dark grey) groups was tested with the bootstrap-boosted Mann–Whitney *U* test for resting platelets and for each concentration of PAR-4 activating peptide, $^{**}p_{\text{bootstrap}} < 0.02$ or lower; $n = 6$. (b) The sizes of CD61/CD41-positive objects in the subpopulations of normoplatelets (cluster 1) and aggregates (cluster 2) in whole blood samples from nondiabetic and streptozotocin-diabetic mice. The objects were discriminated based on flow cytometry forward scatter data, with the use of the Data Mining-assisted generalized cluster analysis by EM (expectation–maximization) algorithm, which decomposes the overall population into two exponentially modified Gaussian partial distributions relevant to platelet subpopulations representing small objects (normoplatelets, predominantly single blood platelets) and larger objects (platelet aggregates with other blood cells) in nondiabetic (light grey) and STZ-induced diabetic (dark grey) mice. Object sizes were estimated from the standard curve assigned with FSC calibration beads (size range of 1 μm to 15 μm). The contributions of normoplatelets and aggregates were 77.6% *vs*. 22.4% in nondiabetic and 50.6% *vs*. 49.4% in STZ-diabetic animals ($p < 0.0001$ for aggregates: 22.4 ± 3.1% in control *vs*. 49.3 ± 9.1% in diabetic mice, bootstrap estimate of an unpaired Student's *t*-test, 1000 iterations). (c) The relative fraction of vWF-positive platelets in pools of "normoplatelets" and "aggregates" in nondiabetic (left) and STZ-diabetic mice (right). Results shown as median (horizontal line) with interquartile range (box) and raw data, $^{***}p < 0.001$, $n = 9$.

support firm interaction of platelet GPIIb/IIIa with its ligand on the vascular wall. It is thus obvious that the pattern of interaction of platelets with the endothelium in pathological conditions is associated with the type of metabolic disorder, the type of vascular bed and possibly with the severity of the endothelial dysfunction.

This hypothesis can be supported by the similar findings derived from a model of acute activation of intact endothelium in the mesentery vasculature in mice. In mouse mesenteric venules stimulated with calcium ionophore A23187, platelet adhesion was found not to be dependent on GPIIb/IIIa, as the wt platelets and the platelets lacking β3 integrin were found to adhere equally efficiently [26]. Interestingly, A23187-stimulated adhesion was absent in vWF–/– mice, which clearly indicated that the degree of GPIb binding to vWF fully accounted for the interaction with vascular wall. In addition, topical application of the ionophore resulted in a rapid accumulation of adhering platelets, and these platelets detached shortly after the cessation of stimulation. The authors deduced that the adhesion events were not sufficient to develop firm adhesion of platelets stabilized by GPIIb/IIIa. Their immunohistochemistry analysis found the endothelium of venules remained intact after treatment with the ionophore. Similarly, our findings did not reveal the presence of any significant deterioration of the endothelial layer. Thus, the endothelium of the mesentery in mice with 1-month diabetes resembles the platelet adhesion conditions generated by transient activation, resulting in the mobilization of endothelial vWF pool.

In line with these expectations, we have detected higher expression of vWF in the endothelium of mesenteric vessels of STZ mice. Interestingly, this was not associated with increased levels of circulating vWF in the plasma of STZ mice. These apparently contradictory results can be explained by another finding: flow cytometry analysis revealed a significantly higher pool of vWF positive platelets in STZ mice, most of which were in the aggregates fraction. This, along with the microscopic observations of the events resembling blood platelets forming strings on vWF in STZ mice, could suggest that platelets could rapidly bind to vWF secreted by and immobilized on the endothelium. Further, once vWF undergoes the

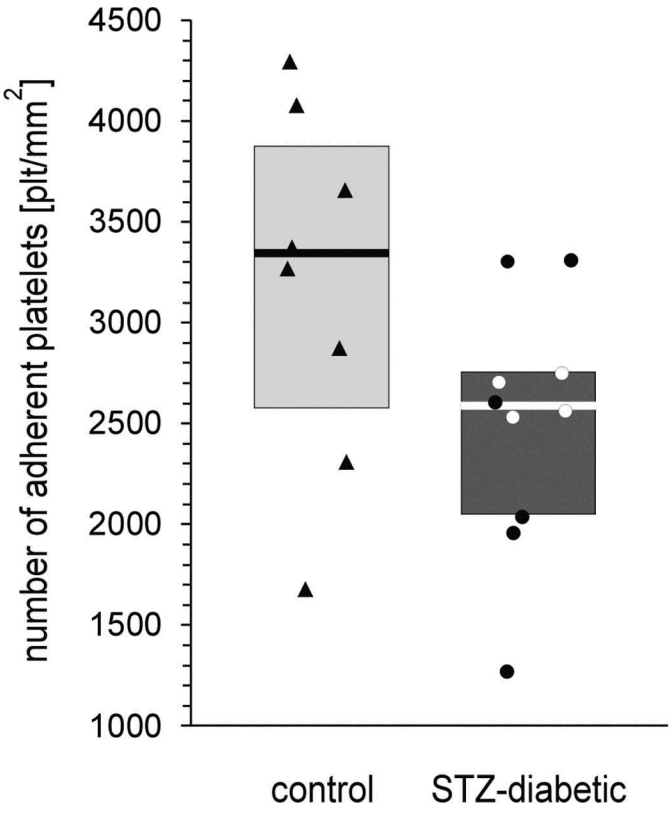

Figure 6. Number of blood platelets of control and STZ mice adhered to von Willebrand factor under flow conditions. Results shown as median (horizontal line) with interquartile range (box) and raw data. Significance of differences tested with Mann–Whitney test, $n = 8$ for control mice and $n = 10$ for STZ mice.

fragmentation mediated by the action of ADAMTS-13, the aggregates of platelets rich in vWF may have become released, as it has been described previously in other models of the endothelial activation [18, 19, 27]. Due to this phenomenon, an excessive amount of vWF released by the activated endothelium in STZ mice circulates as being bound to platelets rather than as a free soluble form and its increased levels in plasma are not detected. At the same time, it has to be kept in mind that some fraction of platelet-bound vWF could also be a portion of the protein secreted from platelets that had undergone activation in a circulation. In our experiments, the stimulation of platelets with PAR-4 activating peptide in plasma-depleted blood, where presumably only traces of vWF were present, resulted in a significant increase in platelet-bound vWF, which suggests that platelets activated in a circulation could release vWF and could be detected as vWF-positive. Until now, however, there is no way to discriminate between the two pools of vWF with the use of flow cytometry. Apparently, increased vWF expression on the platelet surface in diabetic animals is a marker of platelet activation or endothelial dysfunction. Further investigation of the source of vWF on platelets in diabetes and other pathologies could be an interesting step toward improving our knowledge in the field of markers of vascular dysfunction. This would, however, demand novel tools such as antibodies specific against platelet-derived vWF.

It has been shown that vWF in the patients with diabetes underwent carbonylation, which was associated with thrombotic complications, and that the level of high molecular weight multimers of this protein was also increased [28]. Thus, it can be taken into consideration that not only the increased deposition of vWF on endothelium in diabetic mice, but also an altered structure of the protein contributed to the enhanced interaction of platelets with vascular wall. We could not perform the analysis of a structure of vWF bound to the endothelium in the STZ mice. In turn, we made an attempt to evaluate the ability of the binding of plasma soluble pool of vWF to normal platelets in a ristocetin assay. This experiment did not reveal any significant difference in a functionality of a soluble vWF between STZ-diabetic and nondiabetic animals. However, as it has been stated above, we hypothesize that the plasma soluble fraction of vWF may not be representative for the vWF pool secreted by the activated endothelium.

Finally, we also evaluated whether platelets from the STZ-diabetic animals were more prone to interact in flow conditions with the immobilized vWF. This functional assay did not reveal such a tendency. Taking into account the fact that platelets in STZ mice presented higher levels of the activated GPIIb/IIIa receptor and were more reactive, the lack of their enhanced interactions with the immobilized vWF suggests that alterations in platelet function do not explain their enhanced interactions with vessel wall observed *in vivo*. This once again points at an important role of vWF present on the activated endothelium of the STZ mice.

There is yet another factor, which can also explain an increased affinity of blood platelets to the endothelium in diabetes. Recent studies revealed that streptozotocin-induced diabetes in rats increased blood viscosity already 3 days after an onset of diabetes [29]. It is of special interest in terms of the interaction between GPIb receptor with vWF. It has been shown that rolling velocity of blood platelets on vWF decreases with the increase of wall shear stress within its physiological range [30]. Since shear stress increases with an increase of fluid viscosity, the rheological changes in blood in the STZ animals may also contribute to an enhanced interaction of platelets with vWF deposited on the endothelium. Whether an altered blood viscosity really contributed to the rheological changes in blood in the STZ animals in this particular case remains obscure, as far as the putative contributions of various factors influencing such a viscosity (glucose, fibrinogen), although supported by a literature, were not examined in this study and hence, their roles remain rather elusive.

Lowered concentration of insulin in STZ model of diabetes add some complexity to the understanding of the mechanisms of the observed phenomena, as insulin acts in an opposite way on the main components described in the paper. It has been shown that insulin increased platelet activation [31] and that lack of insulin signaling decreased the activation of platelets [32, 33]. On the other hand, insulin stimulates expression of endothelial nitric oxide in endothelial cells [34] and maintains endothelial function [35, 36]. Interestingly, concentrations of IGF-1, another protein from insulin family, which also has a receptor on platelets, were increased in 4-week STZ-diabetes mice and signaling through this receptor enhanced platelet hyperreactivity in these mice [37]. The phenotype which we observed in our model could be a direct effect of an altered insulin signaling or it can be a consequence of hyperglycemia. We do not have a firm evidence at present which particulate factor exhibited the largest contribution in our model: whether it was hyperglycemia or other concurrent factors encountered in diabetic state. The elucidation of the mechanisms leading to the occurrence of this particular phenotype was beyond the scope of the presented study, but remains a subject of our currently performed research.

To summarize, we conclude that platelets interact more frequently with the mesenteric vascular bed in mice with 1-month

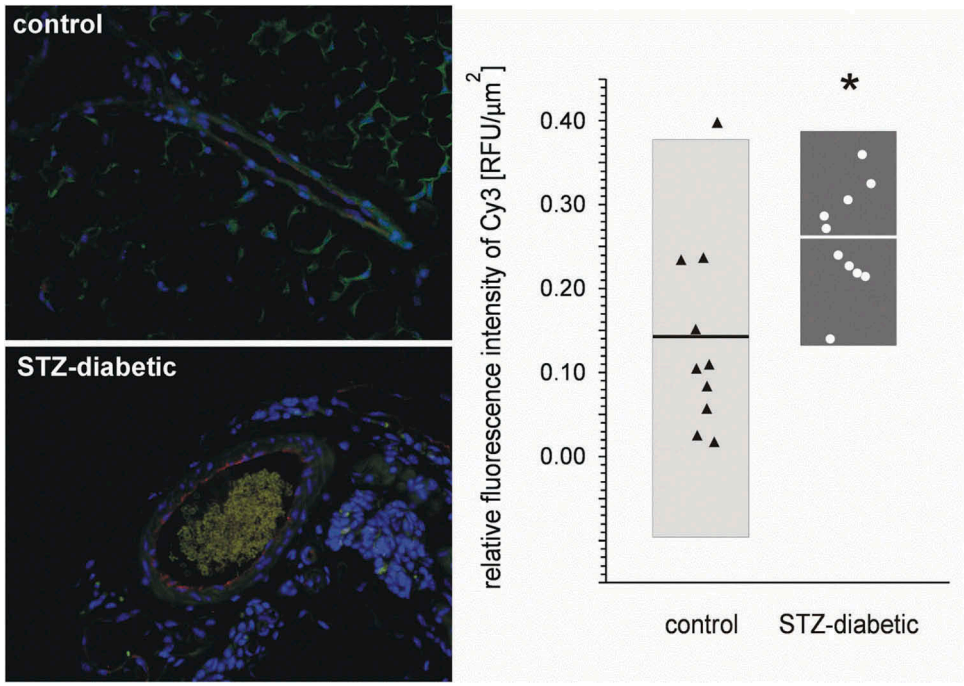

Figure 7. Representative images showing immunofluorescent staining of vWF in mesenteric blood vessels. At least three sections in each mouse were imaged. Green represents unspecific background autofluorescence, blue represents nuclei (Hoechst 33258), and red represents vWF (Cy3). Quantification was performed with the use of AxioVision software (Carl Zeiss, Oberkochen, Germany). Cy3 fluorescence intensity was divided by a vessel lumen area. Results shown as mean (horizontal line) with standard deviation (box) and raw data. Significance of differences tested with bootstrap-boosted unpaired one-tailed Student *t*-test. $^*p_{\text{bootstrap}} < 0.03$, $n = 10$.

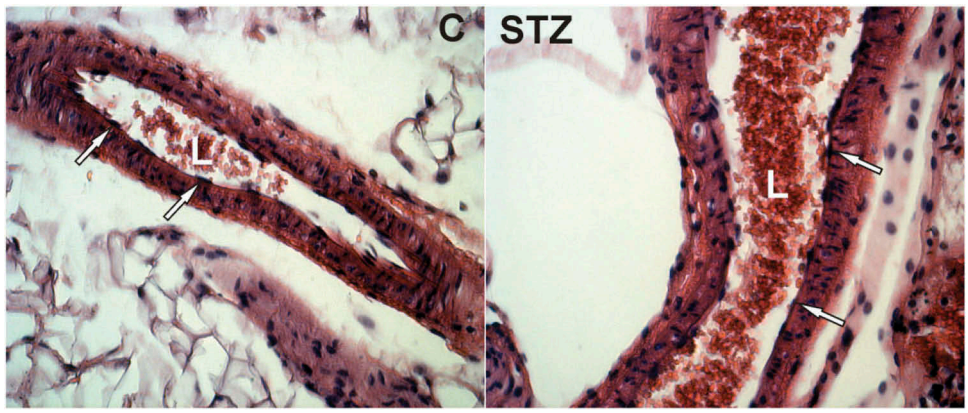

Figure 8. Histological analyses of mesenteric vessels in control and streptozotocin-injected (STZ) mice. L – lumen of the vessel. Arrows indicate the endothelial layer. Dark blue staining shows flat nuclei. The endothelial layer is non-disturbed, it lacks marks of cells detaching from basement membrane.

STZ-induced diabetes than in healthy mice. These interactions are mediated via platelet GPIb-IX-V and are driven by increased expression of vWF in endothelial cells.

Acknowledgments

We express our great thanks to prof. Nieswandt from the Department of Experimental Biomedicine, University of Würzburg, University Hospital and Rudolf Virchow Center, Würzburg, Germany and Emfret Analytics (Eibelstadt, Germany) for the kind gift of Fab fragments of monoclonal anti-GPIbα antibodies Xia.B2 clone and anti-GPIIb/IIIa Leo.H4 clone.

Declaration of interest

The authors report no conflicts of interest.

Funding

This work was supported by the National Science Centre grant MAESTRO (No. DEC-2012/06/A/NZ5/00069). Marcin Talar was supported by Polish National Science Center from grant number UMO-2015/16/T/NZ3/00170.

References

1. Buerkle MA, Lehrer S, Sohn HY, Conzen P, Pohl U, Krotz F. Selective inhibition of cyclooxygenase-2 enhances platelet adhesion in hamster arterioles in vivo. Circulation 2004;110:2053–2059
2. Frenette PS, Moyna C, Hartwell DW, Lowe JB, Hynes RO, Wagner DD. Platelet-endothelial interactions in inflamed mesenteric venules. Blood 1998;91:1318–1324

3. Huo Y, Schober A, Forlow SB, Smith DF, Hyman MC, Jung S et al. Circulating activated platelets exacerbate atherosclerosis in mice deficient in apolipoprotein E. Nat Med 2003;9:61–67
4. Massberg S, Enders G, Leiderer R, Eisenmenger S, Vestweber D, Krombach F et al. Platelet-endothelial cell interactions during ischemia/reperfusion: The role of P-selectin. Blood 1998;92:507–515
5. Pircher J, Merkle M, Wornle M, Ribeiro A, Czermak T, Stampnik Y et al. Prothrombotic effects of tumor necrosis factor alpha in vivo are amplified by the absence of TNF-alpha receptor subtype 1 and require TNF-alpha receptor subtype 2. Arthritis Res Ther 2012;14:R225
6. Massberg S, Brand K, Gruner S, Page S, Muller E, Muller I et al. A critical role of platelet adhesion in the initiation of atherosclerotic lesion formation. J Exp Med 2002;196:887–896
7. Ferreiro JL, Gomez-Hospital JA, Angiolillo DJ. Platelet abnormalities in diabetes mellitus. Diab Vasc Dis Res 2010;7:251–259
8. Henry ML, Davidson LB, Wilson JE, McKenna BK, Scott SA, McDonagh PF et al. Whole blood aggregation and coagulation in db/db and ob/ob mouse models of type 2 diabetes. Blood Coagul Fibrinolysis 2008;19:124–134
9. Paul W, Queen LR, Page CP, Ferro A. Increased platelet aggregation in vivo in the Zucker Diabetic Fatty rat: Differences from the streptozotocin diabetic rat. Br J Pharmacol 2007;150:105–111
10. Rozalski M, Kassassir H, Siewiera K, Klepacka A, Sychowski R, Watala C. Platelet activation patterns are different in mouse models of diabetes and chronic inhibition of nitric oxide synthesis. Thromb Res 2014;133:1097–1104
11. Siewiera K, Kassassir H, Talar M, Wieteska L, Watala C. Higher mitochondrial potential and elevated mitochondrial respiration are associated with excessive activation of blood platelets in diabetic rats. Life Sci 2016;148:293–304
12. Siewiera K, Kassassir H, Talar M, Wieteska L, Watala C. Long-term untreated streptozotocin-diabetes leads to increased expression and elevated activity of prostaglandin H2 synthase in blood platelets. Platelets 2016;27:203–211
13. Jenkins MJ, Edgley AJ, Sonobe T, Umetani K, Schwenke DO, Fujii Y et al. Dynamic synchrotron imaging of diabetic rat coronary microcirculation in vivo. Arterioscler Thromb Vasc Biol 2012;32:370–377
14. Nacci C, Tarquinio M, De BL, Mauro A, Zigrino A, Carratu MR et al. Endothelial dysfunction in mice with streptozotocin-induced type 1 diabetes is opposed by compensatory overexpression of cyclooxygenase-2 in the vasculature. Endocrinology 2009;150:849–861
15. Przygodzki T, Talar M, Watala C. COX-2-derived prostaglandins do not contribute to coronary flow regulation in diabetic rats: Distinct secretion patterns of PGI(2) and PGE(2). Eur J Pharmacol 2013;700:86–92
16. Przygodzki T, Talar M, Przygodzka P, Watala C. Inhibition of cyclooxygenase-2 causes a decrease in coronary flow in diabetic mice. The possible role of PGE2 and dysfunctional vasodilation mediated by prostacyclin receptor. J Physiol Biochem 2015;71:351–358
17. Meijering E, Dzyubachyk O, Smal I. Methods for cell and particle tracking. In: Imaging and spectroscopic analysis of living cells. Elsevier, 2016. p. 183–200.
18. Chauhan AK, Goerge T, Schneider SW, Wagner DD. Formation of platelet strings and microthrombi in the presence of ADAMTS-13 inhibitor does not require P-selectin or beta3 integrin. J Thromb Haemost 2007;5:583–589
19. De MB, De Meyer SF, Feys HB, Pareyn I, Vandeputte N, Deckmyn H et al. The distal carboxyterminal domains of murine ADAMTS13 influence proteolysis of platelet-decorated VWF strings in vivo. J Thromb Haemost 2010;8:2305–2312
20. Matsuda N, Teramae H, Yamamoto S, Takano K, Takano Y, Hattori Y. Increased death receptor pathway of apoptotic signaling in septic mouse aorta: Effect of systemic delivery of FADD siRNA. Am J Physiol Heart Circ Physiol 2010;298:H92–H101
21. Wang M, Chen M, Ding Y, Zhu Z, Zhang Y, Wei P et al. Pretreatment with beta-Boswellic acid improves blood stasis induced endothelial dysfunction: Role of eNOS Activation. Sci Rep 2015;5:15357
22. Fischetti F, Candido R, Toffoli B, Durigutto P, Bernardi S, Carretta R et al. Innate immunity, through late complement components activation, contributes to the development of early vascular inflammation and morphologic alterations in experimental diabetes. Atherosclerosis 2011;216:83–89
23. Kaplan ZS, Jackson SP. The role of platelets in atherothrombosis. Hematol Am Soc Hematol Educ Program 2011;2011:51–61
24. Schafer A, Alp NJ, Cai S, Lygate CA, Neubauer S, Eigenthaler M et al. Reduced vascular NO bioavailability in diabetes increases platelet activation in vivo. Arterioscler Thromb Vasc Biol 2004;24:1720–1726
25. Nieswandt B, Bergmeier W, Rackebrandt K, Gessner JE, Zirngibl H. Identification of critical antigen-specific mechanisms in the development of immune thrombocytopenic purpura in mice. Blood 2000;96:2520–2527
26. Andre P, Denis CV, Ware J, Saffaripour S, Hynes RO, Ruggeri ZM et al. Platelets adhere to and translocate on von Willebrand factor presented by endothelium in stimulated veins. Blood 2000;96:3322–3328
27. Bernardo A, Ball C, Nolasco L, Choi H, Moake JL, Dong JF. Platelets adhered to endothelial cell-bound ultra-large von Willebrand factor strings support leukocyte tethering and rolling under high shear stress. J Thromb Haemost 2005;3:562–570
28. Oggianu L, Lancellotti S, Pitocco D, Zaccardi F, Rizzo P, Martini F et al. The oxidative modification of von Willebrand factor is associated with thrombotic angiopathies in diabetes mellitus. PLoS One 2013;8:e55396
29. Yeom E, Byeon H, Lee SJ. Effect of diabetic duration on hemorheological properties and platelet aggregation in streptozotocin-induced diabetic rats. Sci Rep 2016;6:21913
30. Yago T, Lou J, Wu T, Yang J, Miner JJ, Coburn L et al. Platelet glycoprotein Ibalpha forms catch bonds with human WT vWF but not with type 2B von Willebrand disease vWF. J Clin Invest 2008;118:3195–3207
31. Yngen M, Li N, Hjemdahl P, Wallen NH. Insulin enhances platelet activation in vitro. Thromb Res 2001;104:85–91
32. Hunter RW, Hers I. Insulin/IGF-1 hybrid receptor expression on human platelets: Consequences for the effect of insulin on platelet function. J Thromb Haemost 2009;7:2123–2130
33. Moore SF, Williams CM, Brown E, Blair TA, Harper MT, Coward RJ et al. Loss of the insulin receptor in murine megakaryocytes/platelets causes thrombocytosis and alterations in IGF signalling. Cardiovasc Res 2015;107:9–19
34. Fisslthaler B, Benzing T, Busse R, Fleming I. Insulin enhances the expression of the endothelial nitric oxide synthase in native endothelial cells: A dual role for Akt and AP-1. Nitric Oxide 2003;8:253–261
35. Haines RJ, Corbin KD, Pendleton LC, Meininger CJ, Eichler DC. Insulin transcriptionally regulates argininosuccinate synthase to maintain vascular endothelial function. Biochem Biophys Res Commun 2012;421:9–14
36. Kobayashi T, Taguchi K, Nemoto S, Nogami T, Matsumoto T, Kamata K. Activation of the PDK-1/Akt/eNOS pathway involved in aortic endothelial function differs between hyperinsulinemic and insulin-deficient diabetic rats. Am J Physiol Heart Circ Physiol 2009;297:–H1775
37. Stolla MC, Li D, Lu L, Woulfe DS. Enhanced platelet activity and thrombosis in a murine model of type I diabetes are partially insulin-like growth factor 1-dependent and phosphoinositide 3-kinase-dependent. J Thromb Haemost 2013;11:–929

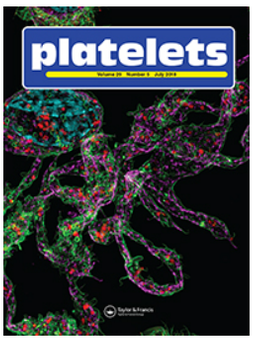

Platelets

ISSN: 0953-7104 (Print) 1369-1635 (Online) Journal homepage: https://www.tandfonline.com/loi/iplt20

Enhanced adhesion of blood platelets to intact endothelium of mesenteric vascular bed in mice with streptozotocin-induced diabetes is mediated by an up-regulated endothelial surface deposition of VWF – *In vivo* study

Tomasz Przygodzki, Marcin Talar, Hassan Kassassir, Lukasz Mateuszuk, Jacek Musial & Cezary Watala

To cite this article: Tomasz Przygodzki, Marcin Talar, Hassan Kassassir, Lukasz Mateuszuk, Jacek Musial & Cezary Watala (2018) Enhanced adhesion of blood platelets to intact endothelium of mesenteric vascular bed in mice with streptozotocin-induced diabetes is mediated by an up-regulated endothelial surface deposition of VWF – *In vivo* study, Platelets, 29:5, 476-485, DOI: 10.1080/09537104.2017.1332365

To link to this article: https://doi.org/10.1080/09537104.2017.1332365